POLITECNICO DI TORINO
Repository ISTITUZIONALE

Preliminary Analysis of the Estimation of Tissue Thermal Parameters for Tumor Laser Ablation with Minimally Invasive Techniques

(Article begins on next page)

11 July 2024

Preliminary Analysis of the Estimation of Tissue Thermal Parameters for Tumor Laser Ablation with Minimally Invasive Techniques

Aurora Bellone
Politecnico di Torino, DET
Torino, Italy
aurora.bellone@polito.it

Elisa Ullo
Politecnico di Torino, DET
Torino, Italy
elisa.ullo@studenti.polito.it

Massimo Olivero
Politecnico di Torino, DET
Torino, Italy
massimo.olivero@polito.it

Gianni Coppa
Politecnico di Torino, DET
Torino, Italy
gianni.coppa@polito.it

Alberto Vallan
Politecnico di Torino, DET
Torino, Italy
alberto.vallan@polito.it

Guido Perrone
Politecnico di Torino, DET
Torino, Italy
guido.perrone@polito.it

Abstract—The optimization of tumor laser ablation requires the evaluation of the temperature distribution in the tumor volume, but minimally invasive sensors can only provide information in one dimension, and often with consistent errors. Therefore, a suitable prediction algorithm, combined with accurate measurements, are required to reconstruct the temperature map in the tumor mass. This work provides preliminary results on the temperature mapping in an agar-gel phantom, using a quasi-distributed temperature sensor made of a fiber Bragg grating array with improved accuracy, and an algorithm of estimation of the temperature spatial distribution based on the thermal Green's function. Details on the fabrication and packaging of the sensor are provided along with an experimental evaluation of the thermal diffusivity in the phantom. Furthermore, it is shown how the accuracy on the evaluation of diffusivity is influenced by the synchronization error, which is the delay between the firing of the laser and the temperature acquisition.

Index Terms—Tumor laser ablation, Thermal parameter of biological tissues, Fiber Bragg grating temperature sensors, Fiber Bragg grating sensor array.

I. Introduction

Minimally invasive high-temperature thermal treatments – the so-called "ablations" – are a set of rather novel therapies for the treatment of solid tumors, which can be used either as adjuvants or as alternatives to more consolidated approaches, such as surgical resection, radiotherapy, or chemotherapy. In particular, thermal treatments of tumors are mostly attractive for patients who are not eligible for traditional surgery. Such treatments require to locally increase the temperature above about $55\,°C$ to ensure the immediate necrosis of malignant cells [1], [2]. Different implementations are described in the literature depending on the heat source, namely radio-frequency, microwave, or laser ablations. Each solution has its own strengths, but they all share the advantage of causing less discomfort to the patient and of implying lower overall costs, being less traumatic and requiring fewer days of hospitalization. In this paper it is specifically addressed the case of Laser Ablation (LA), but many of the conclusions are expected to be straightforwardly applied also to the other heating techniques.

LA uses high-power laser beams, up to about $10\,W$, typically generated by laser diodes emitting in the $905\,nm$ to $980\,nm$ range [3]. In the case of tumors affecting internal organs, the laser beam is delivered using a large core fiber inserted through the skin with a needle, which is accurately positioned via ultrasound image guiding, magnetic resonance or computed tomography [4].

Since the effect of LA is predominantly thermal, it is pretty obvious that optimal outcomes would require measuring the temperature distribution in all the treated area. However, in practical cases this is not possible because to stay within a minimally invasive scenario the temperature can be directly measured only by inserting a temperature sensor through the same needle used for the laser delivery fiber. In other words, the temperature can be measured only in the portion of the tissue along the laser delivery fiber; so, it is basically a one-dimensional measurement when a three-dimensional one would be required.

Sensors based on optical fibers are very good candidates for the measurement of temperature in the biomedical field because they are immune from electrocution and do not exhibit significant self-heating due to interaction with the laser beam (or other electromagnetic sources of radiations, such as microwaves). Moreover, being all-dielectric structures, they are compatible with Magnetic Resonance Imaging (MRI). The most widespread fiber optic temperature sensors are those using Fiber Bragg Gratings (FBGs) [5], which represent a well consolidated technology, with an exceptional balance between sensitivity, robustness, and

fabrication complexity. FBGs have extensively been used to measure the temperature during LA procedures [6]–[8]. An alternative is constituted by interferometric sensor relying on single mode - multi mode - single mode (SMS) structures, which are attractive for their higher sensitivity; however, SMS sensors cannot be used for the applications discussed in this paper because of their intrinsic long length that leads to strong limitations in terms of the achievable spatial resolution [9]. Therefore, in this work temperatures are measured with FBG sensor arrays. An FGB array consists of a cascade of FBGs inscribed along the same fiber, but with slightly different reflection peaks. Multiple FBG arrays can be simultaneously interrogated using a single instrument, hence they can be used to implement a quasi-distributed sensing system with millimeter-size spatial resolution [10]. FBG arrays have already been used to reconstruct the temperature map during tumor thermal treatments [11]; however, in most cases, as in the cited paper, FBG arrays are disposed to form grids around the applicator. This is an efficient approach to measure the obtained temperature distribution during lab experiments, but it is hardly applicable during actual surgeries, unless the minimally invasive requirement is released and with an increase in the patient discomfort.

In previous papers we demonstrated the possibility of combining laser delivery with temperature sensing capabilities using FBGs [12], [13]. The challenge thus becomes how to estimate the temperature distribution in the tumor volume from pinpoint temperature measurements along the delivery fiber only. This represents a sort of ill-posed problem, but "good enough" estimates for the intended application can be obtained with prediction algorithms that extend the available measured data through simulations based on combined optical beam propagation and thermal models. In the simplest form, an estimation of the temperature map distribution over the entire area of interest can be obtained by solving a multi-physic model with the constrain that the predicted temperature along the delivery fiber has a good overlap with the measured temperature profile. Other more sophisticated methods can be used, but in any case the starting point is the knowledge of the biological tissue optical and thermal properties. However, these values are difficult to estimate since they cannot be taken from literature data or obtained from previous experiences given the variability typical of biological tissues, not only from individual to individual, but also within the organ itself. Therefore, they must be evaluated from some measurements that have to be conducted directly on the target organ before the ablation procedure. In particular, thermal parameters can be evaluated using the Heat Pulse Method (HPM) [14].

The goal of evaluating the temperature distribution map during a laser ablation procedure without worsening the invasive impact to continuously optimize the laser parameters is very ambitious. In another paper we have already discussed some aspects related to the reconstruction of the temperature map from partial measurements through suitable hyperthermal treatment planning models [15]; in this paper we conduct a preliminary analysis on the requirements that such approach poses to the measurement quality. In more detail: i) we investigate the accurate characterization of "laser beam compatible" multi-point thermometers made with arrays of FBGs to measure the temperature along the beam delivery fiber; ii) we discuss the impact of synchronization errors between the switching on and off of the laser and temperature acquisitions on the application of the HPM to recover the thermal parameters.

Measuring the temperature during medical treatments, such as the mentioned tumor laser ablation, does not usually poses stringent requirements from the metrological viewpoint since errors in the order of $\pm 0.5\,°C$ are acceptable. However, in the cases considered in this paper this is no longer true because the measured temperature in a specific location is used to reconstruct a temperature map that extends well around that location and in this process errors gets amplified. Therefore, to obtain meaningful results it is necessary to lower as much as possible the error, hopefully below $\pm 0.1\,°C$. Contrary to conventional sensors (e.g., thermistors or thermocouples for which this target value is commonly achieved; but these devices cannot be used with lasers due to their self-heating), this requirement represents a real challenge for FBG thermometers and requires special care in the fabrication and calibration of the sensors.

II. FBG TEMPERATURE SENSORS

As already pointed out, despite other types of fiber optic sensors may exhibit larger sensitivity, the necessity of a shorter gauge length and the possibility of spatial multiplexing to fabricate thermometer arrays have led to the choice of FBG-based sensors for the measurement of the temperature both for the implementation of the HPM and for real-time measurement of temperature during the laser ablation procedure. Therefore, to this purpose, *ad-hoc* optical fiber sensors have been developed and realized.

A. Fiber Bragg Grating fabrication

FBGs are a periodic refractive index modulation inscribed in the core of a fiber, obtaining a device with a notch-like filter behavior, in which the deep spectral position, the so-called Bragg wavelength, depends on the local temperature and the applied strain. Traditionally, FBGs are fabricated exposing a special photosensitive fiber to an intense UV laser diffracted through a phase mask. In this case the Bragg wavelength is set by the pitch of the phase mask, which determines the periodic intensity pattern of the UV beam on the fiber and, in turn, the periodic refractive index modulation. More recent FBG fabrications, instead, employ a femtosecond laser inscription [16]; this is the choice we made for the thermometers here presented, since it simplifies the fabrication of arrays. The physics behind this technique is different from the UV
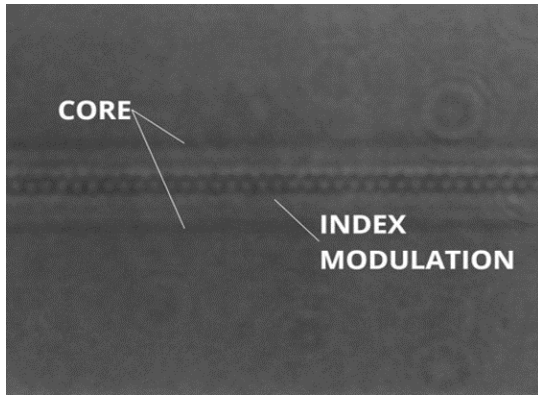
Fig. 1. Micrograph depicting the core of the optical fiber containing an FBG inscribed with point-by-point technique. The pitch of the periodic pattern determines the Bragg wavelength.

Fig. 2. Packaged sensor: array of 13 fiber Bragg gratings in a glass capillary.

inscription and relies on non-linear phenomena produced by ultra-short laser pulses in transparent media [17]. From an application viewpoint, femtosecond laser writing allows FBGs being inscribed in any type of optical fiber, so that photosensitivity of the core and other photo-sensitization techniques are not required; moreover, inscription can be performed without the necessity of phase masks or of any diffractive element. In particular, the sensors used in the experiments hereby presented, were fabricated by point-by-point technique for which the required refractive index modification is obtained by firing the laser in a sequence of spots along the fiber (Fig. 1). This way, each array could be fabricated in a single run, with easy tuning of the writing parameters in order to choose the number of FBGs, the Bragg wavelength, and the length of each FBG (i.e., the sensing length). The result were sturdy and thermally stable FBGs, suitable for applications in harsh environment [18].

The Bragg wavelength λ_B depends on the spatial periodicity of the perturbation Λ as [19]:

$$\lambda_B = 2n_{\text{eff}}\,\Lambda \tag{1}$$

where n_{eff} is the effective refractive index. Temperature and strain affect the spectral response because they both influence the periodicity and the local refractive index, leading to a shift of the Bragg wavelength according to 2:

$$\Delta\lambda_B = \lambda_B(T_0, \epsilon_0) - \lambda_B(T_0 + \Delta T, \epsilon_0 + \Delta\epsilon) \tag{2}$$

The arrays fabricated for this work consist of 13 gratings inscribed in a telecom-grade G.652 compliant optical fiber, each 2 mm-long; the FBGs are spatially recorded with a nonuniform spacing of of 10 mm at the array edges 5 mm in the middle (Fig. 2); the reduced spacing in the middle of the array is conceived for an enhanced spatial resolution in the area where a higher temperature is expected.

B. Sensor packaging

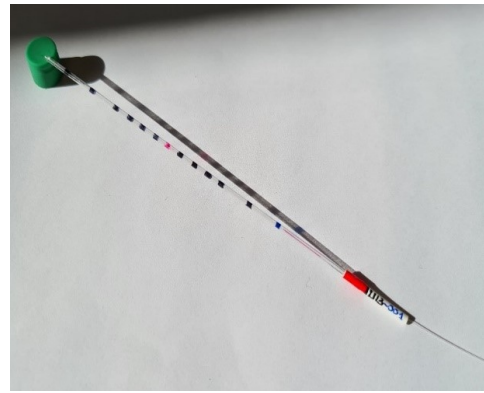As shown in Eq. 2, a cross-sensitivity between temperature and strain is intrinsic in FBG sensors. This can be overcome by mechanically isolating the fiber array from the external environment with a capillary. In the presented thermometers we used a 12 cm-long closed glass capillary, with internal diameter of 1 mm and thickness 0.5 mm, sealed at the end side.

The array is inserted in the glass capillary, leaving the fiber loose and avoiding to touch the end of the capillary. The fiber is fixed at the capillary open side with an optical UV-curable adhesive that also seals the aperture. A picture of the arranged multi-points sensor is shown in Fig. 2, where the ticks on the capillary refer to the positions of the various FBGs in the array.

C. Sensor calibration

The temperature sensors were characterized with a thermally controlled breadboard based on a Peltier-cell (ThorLabs PTC1, dimensions 15 cm to 45 cm). The array under calibration is inserted in a custom made copper holder fixed on the board surface. The holder embeds a reference temperature sensor (4 wire ceramic Pt1000, grade AA) measured with a 6.5 digit multimeter. A thick thermal insulator covers the metallic holder and the top surface of the breadboard and thus it ensures a good temperature uniformity and insensitivity with respect to the ambient temperature.

During the characterization, the Bragg wavelengths of the FBGs in the array are acquired with a commercial FBG analyzer (Luna - Micron Optics si 155, a 4-channel optical interrogator) which is able to track the Bragg peaks at 1 kHz rate. A program written in LabView controls the full characterization procedure and records the current board temperature and the corresponding Bragg wavelength shift. Data are finally processed with a Matlab script that returns the calibration constants and the calibration error for each FBG sensor.

Using this setup a single array can be automatically calibrated from 15 °C to 45 °C in about one hour.
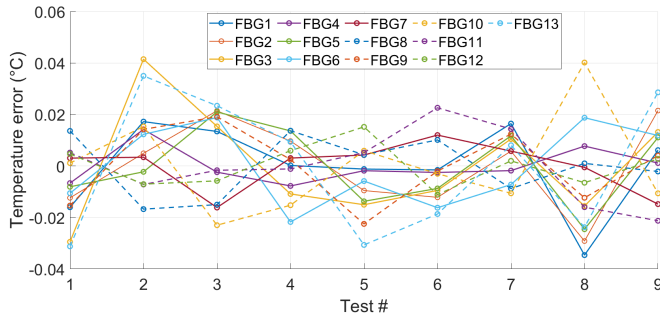
Fig. 3. Temperature error of the developed 13-FBG array sensor.

Fig. 4. Temperature response to a heat pulse for various distances from the heat source.

D. Calibration results

The calibration constants of each FBG have been obtained with the setup described in Sect.II-C using a polynomial fitting of the recorded data (FBG temperature and corresponding Bragg wavelength). As an example, Fig. 3 shows the residual fitting error for a capillary containing 13 FBGs.

Thanks to a careful fabrication procedure, the residual error is below $\pm 0.05\,°\text{C}$, a value that represents a remarkable improvement with respect to off-the-shelf commercial FBG-based sensors. Moreover, it makes the developed thermometer array suitable for the measurement of low thermal gradients like in the case of microwave induced hyperthermia. The overall sensor uncertainty is still under investigation because some contributions, such as the effect of FBG spectral distribution and thermal effect of the capillary have not been evaluated yet. These are not easy to quantify since there is no standard procedure for this assessments, but our research is ongoing.

III. Estimation of thermal parameters

The heat pulse method is based on the experimental evaluation of the thermal impulse response function – also called the thermal Green's function – and in its use to estimate the tissue thermal parameters by fitting the measurements to the theoretical expression. Theoretically, the Green's function would require a delta function source, both in time and in space, which is clearly unfeasible. However, analytical expressions can be found also for sources having Gaussian space distribution. Considering a spatially Gaussian heat pulse:

$$q(\tilde{x}, t) = Q\,\delta(t)\,\frac{1}{(2\pi\sigma_\text{s}^2)}\,\exp\left(-\frac{r^2}{2\sigma_\text{s}^2}\right) \qquad (3)$$

where Q is the heat source, σ_s is the spatial width of the Gaussian heat source, and r is the distance from the source, assuming a homogeneous medium (although this is an approximation in a real scenario) and a 2D case we obtain the temperature distribution for $t \geq 0$:

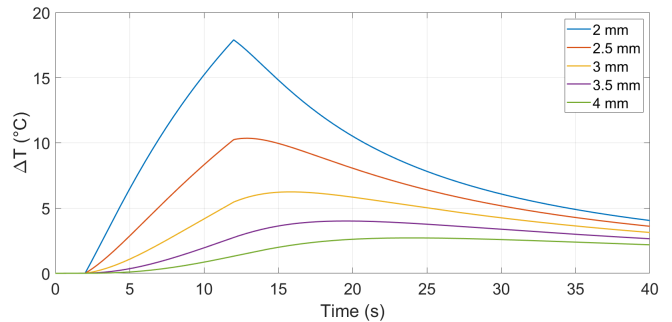$$T(r, t) = Q\int_{t_s}^{t+t_s}\frac{1}{\{4\pi\alpha\tau\}^{3/2}}\,\exp\left(-\frac{r^2}{4\alpha\tau}\right)\mathrm{d}\tau \qquad (4)$$

where $\sigma_\text{s}^2 = 2\alpha\,t_\text{s}$, being:

$$\alpha = \frac{k}{\rho\,C}$$

the thermal diffusivity, C the heat capacity of tissue, ρ the tissue density, and k the thermal conductivity.

In the experimental implementation, the laser is switched on for a relatively short time (order of seconds), enough to induce a heat source due the absorption by the tissue, causing an increase in the temperature, which is followed by a decrease to the original initial temperature after the laser is switched off.

The delay between the laser switching on and the start of the temperature change increases as the distance from the source increases, while the maximum temperature decreases, both depending from the thermal parameters, as shown in the example reported in Fig. 4. Therefore, proper fitting between the measured temperature variation and the results of Eq. 4 requires accurate synchronization between the laser trigger and the temperature acquisition.

Clearly, the larger the number of fitting points, the more accurate will be the estimation of the parameters: for this reason, in the experiments the temperature was recorded during both the heating and cooling phases and, taking advantage of the FBG arrays, in multiple points and at different distances from the fiber delivery tip, which represents the heat source.

A. Evaluation of the tissue thermal parameters

The developed sensors were then used for the estimation of the thermal parameters, starting from the application to an agar-gel phantom made by boiling some agar-agar powder in water, loaded with black ink and lipids to better mimic the liver tissue. This mock-up constitutes a reference case that allows estimating the errors in the parameter reconstruction method since it is expected that its thermal properties are very close to that of water. For this, the phantom was heated with a 2 W-915 nm laser source for up to 10 sec. The experiment was repeated several times in slightly different conditions. In particular, the procedure was repeated measuring the temperature at different distances. To properly position the FBG sensor
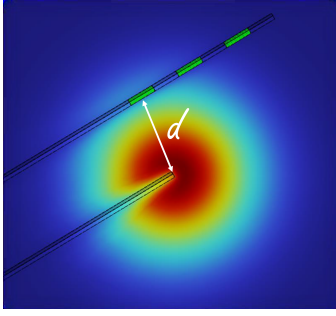
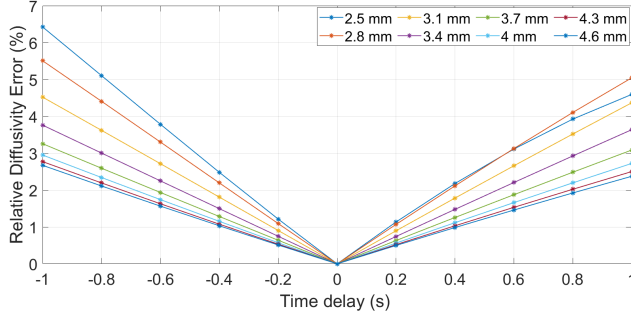Fig. 5. Positioning of the fiber sensor with respect to the laser source probe at distance d.

Fig. 6. Error in the reconstructed thermal diffusivity for the different synchronization errors, at different distances from the source.
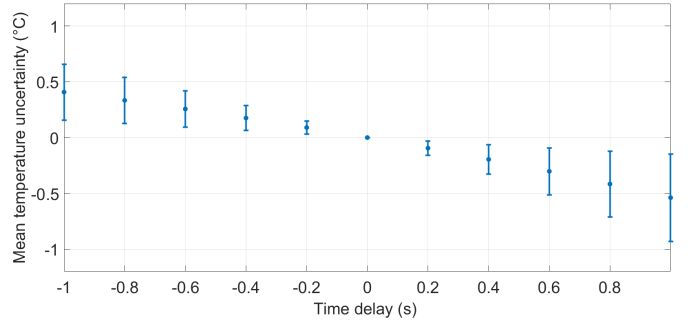

Fig. 7. Error in the estimated tissue temperature, due to the error in the estimation of the thermal diffusivity parameter shown in Fig. 6. The error bars take into account the distances of the sensing point from the heat source.

array with respect to the laser delivery fiber, the agar mock-up was made by two overlapped slices to allow positioning the fibers while open. The sensor was placed at a distance d from the source, as depicted in Fig. 5, resulting in distance ranges for the various sensors in the array from 2.5 mm to 4.6 mm.

The laser source and the acquisition system were controlled through a LabView program. The considered delays are both positive and negative, with absolute values: 0.2 s, 0.4 s, 0.6 s, 0.8 s, and 1 s.

After the fitting between the measured thermal transient and the analytical expression of the temperature from the Green's function, the thermal diffusivity was estimated.

B. Synchronization error effects

The synchronization between the switching on of the laser and the temperature acquisition turned out to play a major role in determining the errors of the recovered parameters. For example, Fig. 6 shows the error (with respect to the value of water) on the value of the reconstructed thermal diffusivity against the synchronization delay for different distances between the sensor and the heat source. While the error is negligible for optimal synchronization, the maximum relative error grows up to about 6.4%.

The consequence of the error on the thermal diffusivity due to synchronization translates into an uncertainty in the measured temperature ranging between 0.41 °C and −0.54 °C, as shown in Fig. 7.

C. Temperature profile reconstruction

The evaluated thermal parameters allow predicting the temperature distribution during a laser ablation treatment. As a preliminary assessment of this capability we used the readings of a temperature sensor of an FBG array to recover the thermal parameters, from which we estimated the temperature evolution in another sensing point. The experimental setup is similar to that shown in Fig. 5 in which the heat source is a 600 µm multi-mode optical fiber. The sensor array is positioned 3 mm from the laser delivery fiber and is composed of FBGs with 5 mm separation from each other. The agar gel phantom was heated with a 5 W-laser source for 5 s; the thermal diffusivity was evaluated in the position closer to the laser source and then used to reconstruct the thermal evolution at the following sensing point located 5 mm away. Fig. 8 compares the acquired and reconstructed temperature profiles at the two sensing points. The inset shows a detail to evidence that the very good agreement between the measured data and the outcomes of the theoretical model. The difference between the temperature profile measured 5 mm from the sensing point used to evaluate the thermal parameters and the predicted profile is well within the acceptable tolerances. Therefore, despite being only a preliminary experiment carried out in a phantom, the results can be considered encouraging for the applicability of the developed procedure.

IV. Conclusion

Multi-point sensors made with FBG arrays were developed and characterized for monitoring the spatial distribution of temperature during hyperthermal treatments of tumors. This activity is part of a larger project that focuses on the development of a tumor ablation planning tool. The ultimate goal is to optimize mini-invasive surgical treatments, ensuring that the cytotoxic temperature values are reached over the entire cancer mass while avoiding charring. The developed sensor consists of a cascade of FBGs, inscribed in a standard telecom fiber with a femtosecond laser. The sensing fiber is packaged in
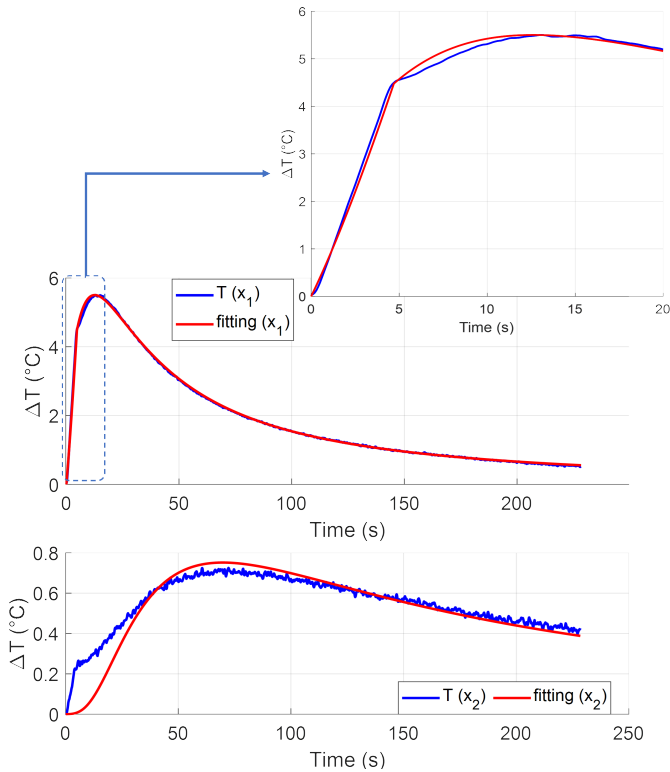
Fig. 8. Upper plot: comparison between the measured temperature (blue) and the fitting with the model (red) in the sensing point used to evaluate the thermal parameters. Lower plot: comparison between the measured temperature (blue) and the predicted profile (red) in a sensing point located 5 mm away.

a glass capillary for an enhanced mechanical protection. The accurate manufacturing results in a temperature error below $\pm 0.1\,°C$, which is better than the performance of commercial sensors of the same type. This is required to accurately reconstruct a temperature map around the laser applicator starting from the values measured along a parallel optical fiber. Besides the fabrication and characterization of the temperature sensors, the work also introduced the estimation of the thermal properties of a biological tissue using the heat pulse method. In particular the analysis focused on the synchronization error between the activation of the laser beam and the temperature acquisition. The experiments carried out with agar gel phantoms demonstrated the possibility to estimate the thermal parameters with negligible error only for a negligible synchronization error. A quantitative experimental analysis showed that the synchronization error must be kept below $\pm 1\,s$ in order to ensure an acceptable temperature uncertainty of $\pm 0.5\,°C$. Preliminary experiments were also conducted to assess the capability of the proposed approach to accurately reconstruct the temperature evolution in points surrounding that used to recover the tissue thermal parameters.

REFERENCES

[1] C. Brace, "Thermal tumor ablation in clinical use", *IEEE Pulse*, pp. 28–38, 2011.
[2] C. J. Diederich, "Thermal ablation and high-temperature thermal therapy: Overview of technology and clinical implementation," *International Journal of Hyperthermia*, vol. 21, pp. 745–753, 2005.
[3] P. Saccomandi, G. Quero, et al., "Laser ablation of the biliary tree: in vivo proof of concept as potential treatment of unresectable cholangiocarcinoma," *International Journal of Hyperthermia*, vol. 34, pp. 1372–1380, 2018.
[4] M. Ahmed, C. L. Brace, F. T. Lee, and S. N. Goldberg, "Principles of and advances in percutaneous ablation," *Radiology*, vol. 258, pp. 351–369, 2011.
[5] W. Chen, R. Gassino, et al., "Performance assessment of FBG temperature sensors for laser ablation of tumors,"*Proc. IEEE International Symposium on Medical Measurements and Applications (MeMeA)*, 2015.
[6] E. Schena, D. Tosi, P. Saccomandi, E. Lewis, and T. Kim, "Fiber optic sensors for temperature monitoring during thermal treatments: an overview," *Sensors*, vol. 16, pp. 1144, 2016.
[7] G. Palumbo, A. Iadicicco, S. Campopiano, et al., "Measurements of temperature during thermal ablation treatments on ex vivo liver tissue using fiber Bragg grating sensors," *2017 IEEE International Instrumentation and Measurement Technology Conference (I2MTC)*, pp. 1-6, 2017.
[8] S. Korganbayev, A. Orrico, L. Bianchi,et al., "Closed-loop temperature control based on fiber Bragg grating sensors for laser ablation of hepatic tissue," *Sensors*, vol. 20 pp. 6496, 2020.
[9] M. Olivero, A. Vallan, R. Orta, and G. Perrone, "Single-mode-multimode-single-mode optical fiber sensing structure with quasi-two-mode fibers", *IEEE Trans. Instr. Meas.*, vol. 67, pp. 1223 − 1229, 2018.
[10] A. Beccaria, A. Bellone, et al., "Temperature monitoring of tumor hyperthermal treatments with optical fibers: comparison of distributed and quasi-distributed techniques", *Optical Fiber Technology*, vol. 60, pp. 102340, 2020.
[11] G. Palumbo, E. De Vita, E. Schena, et al., "Multidimensional thermal mapping during radiofrequency ablation treatments with minimally invasive fiber optic sensors,"*Biomed. Opt. Express*, vol. 9, pp. 5891–5902, 2018.
[12] Y. Liu, R. Gassino, A. Braglia, et al., "Fibre probe for tumour laser thermotherapy with integrated temperature measuring capabilities", *Electronics Letters*, vol. 52, pp. 798–800, 2016.
[13] R.Gassino, Y. Liu, M. Konstantaki, A. Vallan, S. Pissadakis, and G. Perrone, "A Fiber optic probe for tumor laser ablation with integrated temperature measurement capability", *Journal of Lightwave Technology*, vol. 35, pp. 3447–3454, 2017.
[14] H. He, et al., "Development and application of the heat pulse method for soil physical measurements", *Reviews of Geophysics*, vol. 56, pp. 567 − 620, 2018.
[15] R. Gassino, et al., "Temperature distribution mapping using an FBG-equipped probe for solid tumor laser ablation," *IEEE International Symposium on Medical Measurements and Applications (MeMeA)*, pp. 1–6, 2018.
[16] S.J. Mihailov, et al., "Fiber Bragg gratings (FBG) made with a phase mask and 800 nm femtosecond radiation", *OFC 2003 Optical Fiber Communications Conference*, 2003.
[17] J. He, et al., "Review of femtosecond-laser-inscribed fiber Bragg gratings: fabrication technologies and sensing applications", *Photonic Sens*, vol. 11, pp. 203—226, 2021.
[18] S.J. Mihailov, D. Grobnic, C. Hnatovsky, et al., "Extreme environment sensing using femtosecond laser-inscribed fiber Bragg gratings", *Sensors*, vol. 17, 2017.
[19] T. Erdogan, "Fiber grating spectra", *Journal of Lightwave Technology*, vol. 15, no. 8, pp. 1277-1294, 1997.